# Road Surface Recognition Using Laser Radar for Automatic Platooning

Masahiko Aki, Teerapat Rojanaarpa, Kimihiko Nakano, *Member, IEEE*, Yoshihiro Suda, Naohito Takasuka, Toshiki Isogai, and Takeo Kawai

***Abstract*—This paper proposes a road surface recognition system based on a "laser radar" (LIDER), which is used to detect a lane markings for application to an automatic platooning system for trucks. To ensure the safety of automatic driving, there is a need to recognize the road surface conditions (dry, wet, etc.). This system proposes an integrated system that is not only capable of recognizing lane markings but also monitors the road surface using a laser radar scanning system. Our road surface recognition method relies on the multiple reflection intensities of laser radar and a machine learning algorithm. By using multiple reflection intensities, the recognition rate is improved. Moreover, to improve the recognition rate, an additional feature variable, called the "roughness index," is proposed. In this paper, the concept of a road surface recognition system is proposed and six road surface conditions (dry old asphalt, moist old asphalt, flooded old asphalt, dry new asphalt, moist new asphalt, and flooded new asphalt) are recognized by the proposed algorithm. The quality of the road surface recognition is examined through comparison with long-term measurement data. The proposed method exhibits a high level of road surface recognition performance.**

***Index Terms*—Automatic platooning, condition monitoring, laser radar, road surface recognition, machine learning, safety, field operation test.**

## I. Introduction

In recent years, automatic and autonomous driving technologies have been the focus of considerable research [1], [2]. For example, an automatic platooning technology was developed by the California Partners for Advanced Transportation Technology (PATH) [3] as well as by the CHAUFFEUR project [4]. In addition, automatic platooning technology for trucks was developed by the Trains for Safe Road Environment (SARTRE) [5] and KONVOI [6] in Europe. In Japan, automatic platooning technology for buses, named the Intelligent Multimode Transit System (IMTS) was developed by Toyota Motor Corporation [7].

Fig. 1. Automatic platooning with energy-saving ITS.

In addition, automatic and autonomous driving technologies were developed by Carnegie Mellon University, Stanford University and by various other universities and companies [8], [9].

In addition to realizing automatic platooning to reduce labor costs, this project also set out to improve fuel efficiency by applying Intelligent Transport Systems (ITS) technology. Automatic platooning technology for trucks was developed as part of the "Energy-saving ITS project" [10]. In energy-saving ITS, a reduction in the air resistance by using automatic platooning to minimize the distance between trucks realizes the goal of fuel saving. One of the goals of this project was to provide a practical realization of the technology. A practical scenario of "platooning start and end" was configured, and automatic platooning using four trucks with a four-meter clearance between them was realized [11] (Fig. 1).

To enable the actual operation of the automatic platooning system for the trucks of the energy-saving ITS project, there is a need for a means of controlling the distance between the trucks, which will involve monitoring any changes in the friction coefficient between the road and tires.

To ensure that the trucks can perform an emergency stop, the reliability of the truck braking system [12] and the ability to predict the friction coefficient are both very important factors. If an automatic platooning system that has been developed for trucks is to be seen as being practical, a means of automatically determining the status of the road surface will have to be developed. To handle a sudden change in the road surface from dry pavement to moist, flooded, or icy asphalt, there must be a means of monitoring the frictional coefficient and applying it to the automatic platooning so as to maintain the safety of the platoon. Therefore, several researchers have proposed means of estimating the friction coefficient between the tires and the road [13]–[28]. These researches are classified as two categories.

Manuscript received July 14, 2015; revised November 19, 2015; accepted January 30, 2016. Date of publication April 4, 2016; date of current version September 30, 2016. This work was supported by the New Energy and Industrial Technology Development Organization of Japan. The Associate Editor for this paper was P. Ioannou.

M. Aki was with the Institute of Industrial Science, The University of Tokyo, Tokyo 153-8505, Japan. He is now with the Department of Mechanical Science, Nagoya University, Aichi 464-8603, Japan (e-mail: aki.masahiko@gmail.com).

T. Rojanaarpa was with the Institute of Industrial Science, The University of Tokyo, Tokyo 153-8505, Japan. He is now with DENSO Corporation, Aichi 448-8534, Japan.

K. Nakano and Y. Suda are with the Institute of Industrial Science, The University of Tokyo, Tokyo 153-8505, Japan.

N. Takasuka is with DENSO Corporation, Aichi 448-8534, Japan, and also with Nippon Soken Inc., Aichi 445-0012, Japan.

T. Isogai and T. Kawai are with DENSO Corporation, Aichi 448-8534, Japan.

Color versions of one or more of the figures in this paper are available online at http://ieeexplore.ieee.org.

Digital Object Identifier 10.1109/TITS.2016.2528892

One is to estimate a friction force and a friction coefficient between a road and tires based on a dynamical model of a vehicle and tires using GPS information [13]–[23]. Another is to estimate a road surface condition using non-contact sensors which are a camera, a laser radar (LIDER) etc. [24]–[28]. Researches of an estimation of a friction coefficient between a road and a tire based on the dynamical model are classified as two types [23]. One is based on longitudinal dynamics of the vehicle. Another is based on lateral dynamics of the vehicle. In these researches, a friction coefficient between a road and a tire is estimated to use GPS information and to use a Kalman filter as an observer for the vehicle state. In researches using an on-board camera or an on-board laser radar, road surface states are estimated based on measured road surface data (This is not based on a model based estimation). Moreover, sensor fusion technologies by using several kind of sensors have been developed to improve an estimation accuracy of a friction coefficient or a road surface state [20]. Additionally, the friction project which is to estimate a friction force between a road and a tire have been carried out in Europe [19], [20], [29].

In this paper, we propose a means of detecting changes in the frictional coefficient, by determining whether the road surface is dry/wet (as well as judging the quality of the asphalt). This information on the state of the road surface is intended to be used in the initial steps of our efforts to enable the automatic estimation of road surface quality.

Previously proposed methods have used the reflection intensity of laser radar [30], [31], or the brightness of the road surface [25], using camera-based image recognition [26] as the road surface recognition technology. These non-contact sensors are useful for monitoring the road surface [21]. However, it is very difficult to estimate the road surface conditions using only one sensor. Therefore, a sensor fusion technology that integrates the information being received from multiple sensors is used to ensure the most accurate estimate possible.

Our target is to develop a road surface recognition system, not to enlarge the number of sensor for the automatic platooning system. Our road surface recognition system adopted a laser radar (LIDER) [32], [33] which was used for a lane marking recognition system in the automatic platooning system [30], [31]. Therefore, one laser radar is used for both a lane marking recognition system and a road surface recognition system. As a typical road surface changing situation, there is a suddenly change a road surface from inside a tunnel to outside. In this case, a road surface recognition system has to instantly discriminate changing of road surface. However, it is unable to use a road surface recognition system based on a GPS system because GPS system is not able to use in the tunnel. Moreover, it is difficult to use a road surface recognition system based on cameras because it is suddenly changing of light amount. Therefore, a road surface recognition system based on a laser radar of active sensing system in this situation.

In the energy-saving ITS project, laser radar is applied to the lane recognition system. The reflection intensities obtained with this laser radar could also be used to recognize the state of the road surface. In this project, both lane-marking recognition and road surface recognition were realized through the application of laser radar [30], [31]. It is known that it is possible to measure the features of a road surface by using laser radar [34]–[36].

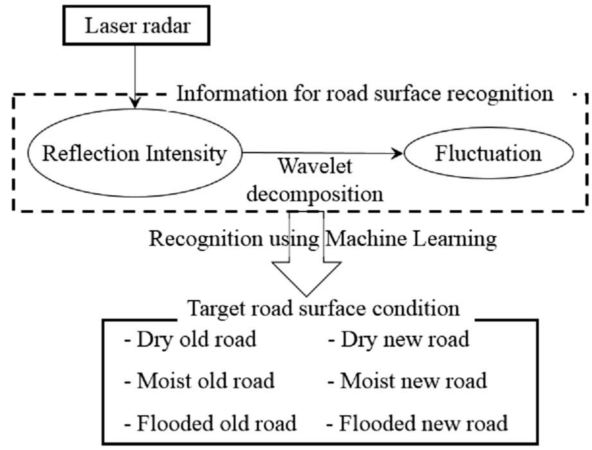


Fig. 2. Concept.

In this study, a road surface recognition technology based on laser radar was developed for application to the automatic platooning system. The proposed algorithm has three main features. First, the relationship between the scanning position and the reflection intensity is approximated by a function using multiple reflection intensities. Second, the naïve Bayes classifier of a machine learning algorithm [37]–[39], which can be applied to variable number-feature amounts, is applied to the variable estimation area to determine whether or not a lane mark is present. Third, to improve the road surface recognition rate, an index indicating the road surface roughness, which is obtained by the wavelet transform of the reflection intensity, is defined as additional information. The multiple reflection intensities and the index of the road surface roughness are used to determine the naïve Bayes classifier.

To verify our proposed algorithm, a long-term measurement test of the road surface was conducted. We were able to achieve a good recognition rate using our proposed algorithm.

## II. Road Surface Estimation Using Laser Radar

### A. Overview of Road Surface Estimation Method

Lane recognition is carried out using laser radar. In our system, the same laser radar is used to monitor the reflection intensity of the lane monitored and the data is fed to the energy-saving ITS technology [30], [31]. Thus, an integrated system that combines lane recognition and road surface state estimation, using information on the reflection intensity of the road surface, can be constructed.

A feature of the reflection intensity of the road surface as measured by laser radar is that mixed data is obtained when performing a single scan of a road section containing both a lane mark and the asphalt surface of the road surface.

The authors are proposing a road surface estimation system that uses the reflection intensity of the road surface and an index of the road surface roughness as obtained by laser radar. This is illustrated in Fig. 2. The index of the road surface roughness is extracted using wavelet decomposition. The road surface state is estimated using a machine learning algorithm.

Conventional road surface estimation systems based on laser radar estimate the road surface state by using a single threshold for the reflection intensity for each road surface state. The authors propose the use of a road surface estimation system, based on laser radar, which uses multiple thresholds of the reflection intensity as determined by the laser radar. Based on the multiple reflection intensity of the laser radar, the mechanical properties of the positional relationship of the reflection of the laser can be regarded as being an approximate functional form. Moreover, a machine learning algorithm is applied to discriminate between the different types of road surface from the multiple thresholds of the reflection intensity. This concept results in a better recognition rate than would be possible with a conventional system. However, it is difficult to maintain a high recognition rate using only the reflection intensities. Therefore, an index of the road surface roughness is derived from the reflection intensities as additional information. The index of road surface roughness is defined as a summation of the irregularities in the reflection intensity in the scanning direction, which is obtained from a wavelet decomposition for classification by a spatial frequency. A road surface estimation is carried out using the naïve Bayes classifier of the machine learning algorithm with the multiple reflection intensities and the index of the road surface roughness. The amount of data for the multiple reflection intensities differs depending on whether or not a lane mark is present as the trucks are progressing along the road. The naïve Bayes classifier is selected as the problem involves a data number that is a time variable.

At this stage, it is only necessary to determine whether the asphalt of the road surface is dry or wet. An estimation problem was set up for six asphalt conditions, to determine data that would be used in this research in the future. These six conditions consisted of combinations of dry, moist, and flooded conditions, as well as new or aged asphalt. A goal of this research was to enable the successful differentiation between the six kinds of asphalt.

### *B. Road Surface Features Determined Using Road Surface Estimation*

*1) Reflection Intensity of Laser Radar:* The reflection intensities of the laser radar differ depending on the road surface, the quality of the road surface and the angles of incidence. Here, the mechanical properties of the reflection intensities are considered.

The laser radar scans the road surface in the transverse and down-facing direction, relative to the vehicles direction of travel. Three points, namely, the reflection of the laser beam from a water film, the absorption of the laser beam by a water film, and the reflection of the laser beam from new and aged road surfaces are considered.

The concept of the reflection of a laser beam by a water film is shown in Fig. 3. The laser beam is reflected in all directions due to the scattering effect of the dry pavement. On the other hand, the laser beam has a directional property when the road surface is covered by a water film, because the surface reflects like a mirror, in addition to there being a scattering effect. Therefore, the reflection intensity decreases at the point furthest from the laser radar, and the reflection intensity increases due to the mirror reflection at points close to the laser radar. The properties of the reflection intensity of the laser radar are shown in Fig. 4.

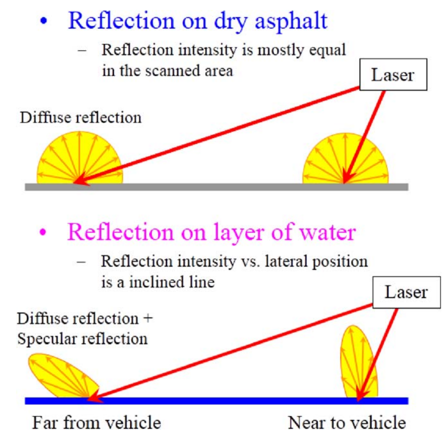


Fig. 3. Characteristics of laser on dry/layer asphalt.

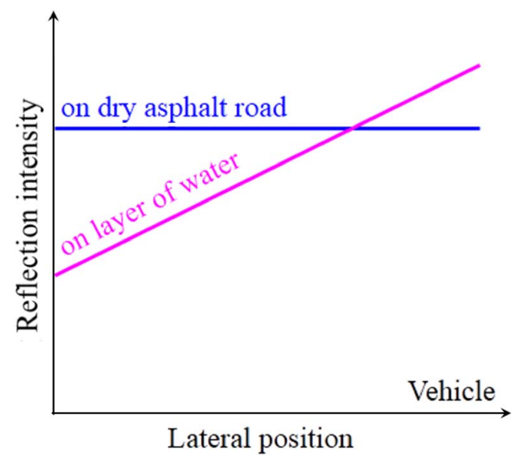


Fig. 4. Reflection intensity on dry asphalt/on layer of water.

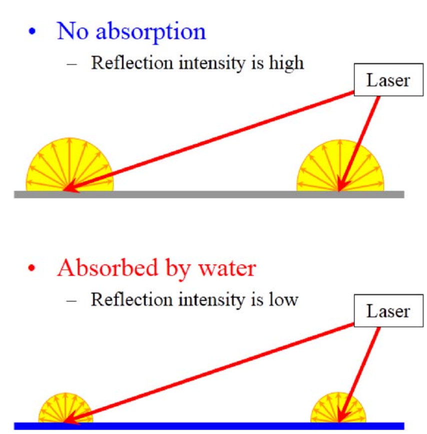


Fig. 5. Characteristics of laser absorption.

The concept of absorption and the reflectance of a laser beam from the water film are shown in Fig. 5. The intensity of a reflection from dry pavement maintains a high value, because there is no water film to absorb the laser beam. On the other hand, when a water film is present, the laser beam

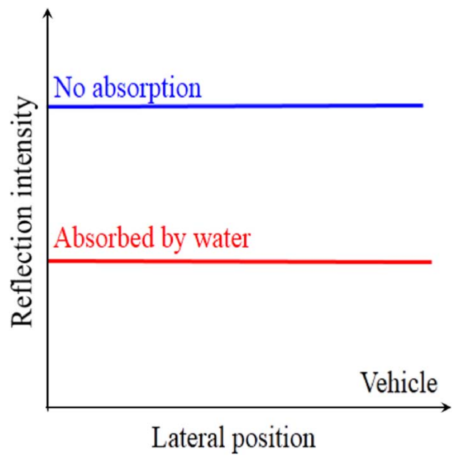


Fig. 6. Reflection intensity by absorption.

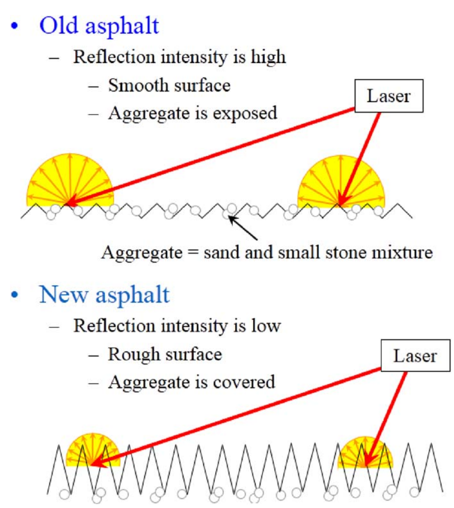


Fig. 7. Characteristics of laser on old/new asphalt.

is absorbed by that film on the road surface at both the far and near positions. Therefore, the reflection intensity decreases more when there is a water film on the road surface than when the pavement is dry. The reflection intensities of the laser radar are illustrated in Fig. 6.

Next, the reflectance property of the laser beam from new/aged asphalt is considered. The concept of the reflection from new/aged asphalt is shown in Fig. 7.

New asphalt is characterized by large grains. These large grains make the new asphalt relatively rough. Once the asphalt ages as a result of the passage of many vehicles over its surface, the asphalt grains become rounded and the road surface overall becomes flattened. Therefore, the reflection intensity of the surface of aged asphalt is greater than that of new asphalt, because the dissipation of the laser beam is reduced by the asperity of the large asphalt grains. The reflection intensities of the laser radar are illustrated in Fig. 8.

Figs. 3, 6, and 8 are reconsidered from the viewpoint of how to differentiate between a moist surface and a flooded surface.

If there is a thin water film on a road surface of aged asphalt (moist asphalt), the reflection intensity is independent of the measurement position relative to the laser radar position and

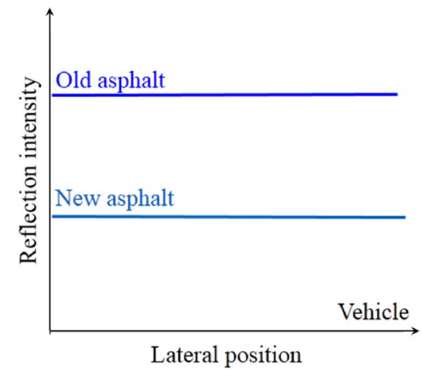


Fig. 8. Reflection intensity on old/new asphalt.

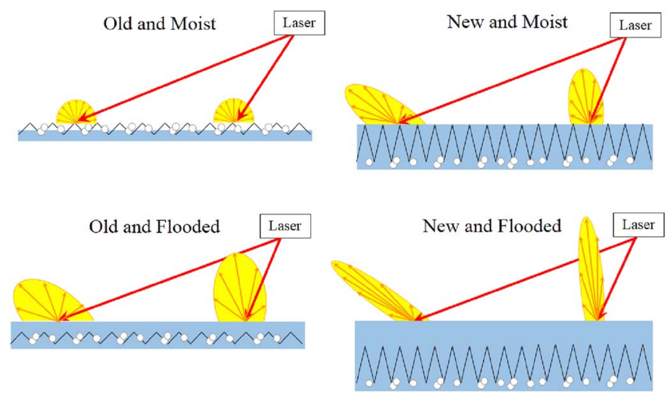


Fig. 9. Characteristics of laser on moist/flooded and old/new asphalt.

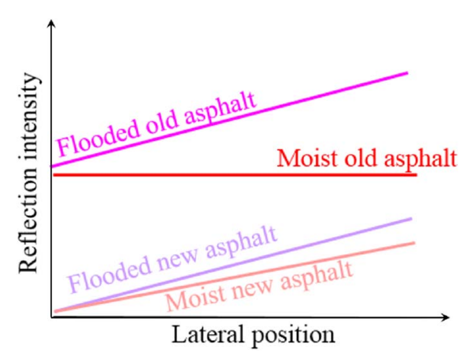


Fig. 10. Reflection intensity on moist/flooded and new/old asphalt.

is constant (Fig. 6). If, however, there is a thick water film on an aged asphalt road surface (flooded asphalt), then the reflection intensity is attenuated at those points that are furthest from the laser radar position, because of the mirror reflection of the laser beam (Fig. 3). On the other hand, the reflection intensity from new asphalt is attenuated more than that from aged asphalt (Fig. 8). Moreover, if the water film on a road surface of new asphalt increases, the attenuation of the rate of reflection intensity from the flooded surface at those points furthest from the laser radar is greater than that from a moist surface because the rate of mirror reflection of the laser beam is large (see Fig. 9).

Based on these findings, the classifications of moist/flooded and new/aged asphalt are as shown in Fig. 10.

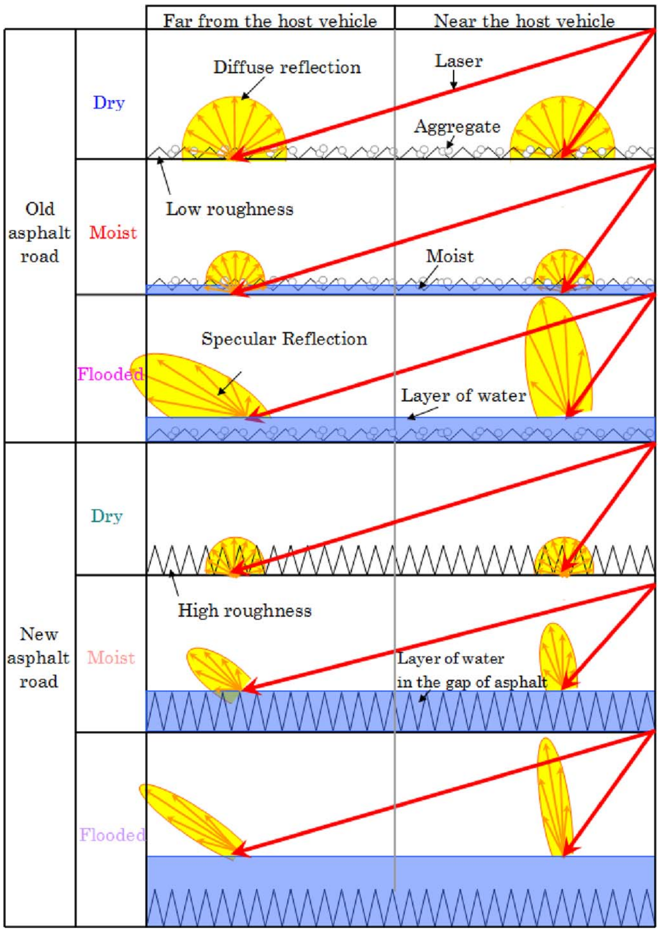


Fig. 11. Mechanical feature of laser reflection.

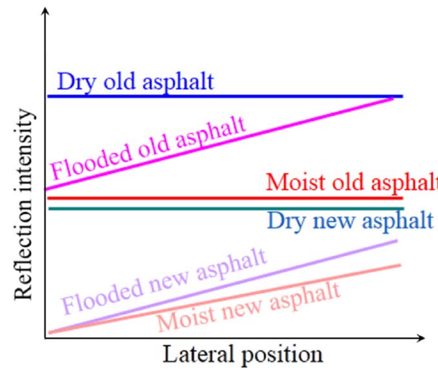


Fig. 12. Summary of reflection intensity.

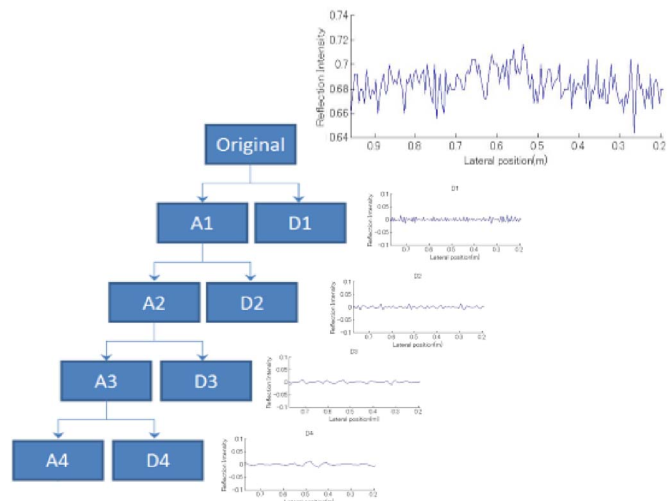


Fig. 13. Concept of roughness distribution.

The obtained results were classified depending on whether the asphalt is dry/moist/flooded and whether the measurement position is far from/near to the laser radar of the vehicle (Fig. 11). Moreover, the relationship between the reflection intensity and the scanning position is shown in Fig. 12. In Fig. 12, the origin point of a coordinate is defined as the farthest position of the scanning range and an abscissa axis is defined from the origin point to the point of the laser radar position. Then, the reflection intensity can be expressed as a function of the position because of the mechanical properties of the road surface.

*2) Index of Road Surface Roughness:* If multiple reflection intensities are only used for a road surface recognition system, there is an envelope to improve a recognition rate. There are similar multiple reflection intensity shapes, like "Moist old asphalt" and "Dry new asphalt" or "Flooded new asphalt" and "Moist new asphalt." Therefore, it is difficult to only use multiple reflection intensities from a laser radar. In order to resolve this problem, a fluidity of multiple reflection intensities with respect to a lateral position is added to new feature quantities. Fluidity of reflection intensity with respect to position is calculated as asperity area from mean value of multiple reflection intensity. And the fluidity is defined as index of road surface roughness. This fluidity shows total amplitude of fluctuation from mean reflection intensity. Because a geometrical asperity of road surface of a new asphalt is larger than a geometrical asperity of road surface of an old asphalt, asperity area of a new asphalt from mean reflection intensity become large. Moreover, asperity area become larger because amplitude of reflection intensity becomes large in sequence of dry asphalt, moist asphalt, and flooded asphalt. The asperity area from mean reflection intensity is defined as index of road surface roughness.

A difference in the reflection angle of the laser beam has its origin in the asperity of the road surface roughness. Therefore, the wavelength component, which is dependent on the asperity of the road surface, is contained in the reflection intensity of the laser radar in the scanning direction. The wavelength component is extracted from the reflection intensity of the laser radar by using the discrete wavelet transform [38], [39]. Fig. 13 shows the procedure for extracting the wavelength components for the road surface. In Fig. 13, at first, the reflection intensity is resolved to a target wavelength component for the road (D1) and a target wavelength-removed reflection intensity (A1) as obtained by the discrete wavelet transform. Second, the A1 data is resolved to a target wavelength component for the road (D2) and a target wavelength-removed reflection intensity (A2) by the discrete wavelet transform. This procedure is continued until the target roughness is extracted.

In this research, the index of the road surface roughness is defined as the summation of the waveband (D1 to D4) containing the target road surface roughness. Therefore, 171 data points for the reflection intensity and one data point for an index of the road surface roughness are obtained in each scan. In addition to multiple reflection intensities, to improve the road surface estimation rate, the index of the road surface roughness is added to the feature quantities for machine learning.

Therefore, index of road surface roughness (IRSR) is defined as a following equation:

$$\mathrm{IRSR} = \sum_{i=1}^{n} \{D_1(i) + D_2(i) + D_3(i) + D_4(i)\}. \quad (1)$$

Here, $n$ denotes a number of multiple points of reflection intensities. $D_1(i)$, $D_2(i)$, $D_3(i)$, and $D_4(i)$ denotes components of a road surface roughness which is calculated from discrete wavelet transformation.

### *C. Road Surface Recognition Based on Naïve Bayes Estimators*

The naïve Bayes classifier is a type of supervised learning used in machine learning algorithms [35]. If the obtained data has a normal distribution in each discriminated class, then naïve Bayes classifier can be used as an effective estimation method.

The following procedure was used to create training data.

1. The reflection intensities obtained from the laser radar and the index of the road surface roughness, as obtained from the discrete wavelet transform of the reflection intensities, were prepared.
2. Feature variable $f_i$, mean value $\mu_i$ and standard deviation $\sigma_i$ $(i = 1, \ldots, N,\ N = n + m)$ are calculated for six classes ("aged asphalt and dry road surface," "aged asphalt and moist road surface," "aged asphalt and flooded road surface," "new asphalt and dry road surface," "new asphalt and moist road surface," and "new asphalt and flooded road surface") which can be clearly identified. Here, $n$ denotes the number of reflection intensity data items obtained from one scan and $m$ denotes the index of the road surface roughness as determined from one scan. In this case, the numbers are $n = 171$, $m = 1$. The reflection intensity data for 171 points is expressed as an approximated function with positions ranging from points that are far from the vehicle to near the vehicle.

When there is no lane in the scanning area, there will be 171 points of multiple reflection intensities in the scanning data. When there is a lane in the scanning area, the reflection intensities of the lane width are excluded from the road surface estimation area. Therefore, the number of feature variables $f_i$ $(i = 1, \ldots, N,\ N = n + m)$ is time-variant. The naïve Bayes classifier can be applied to the time-variant estimation problem in a machine learning algorithm. Therefore, the switching of the estimation area of the road surface is needed either with or without the lane marks in the scanning area. If lane marks exist in the scanning area of the laser radar, they can be separated from the reflection intensities because the lane marks and road surface area can be treated as being independent events using the naïve Bayes classifier. Here, the information for the lane mark area is applied to the results of the lane marking detection algorithm shown in Fig. 14.

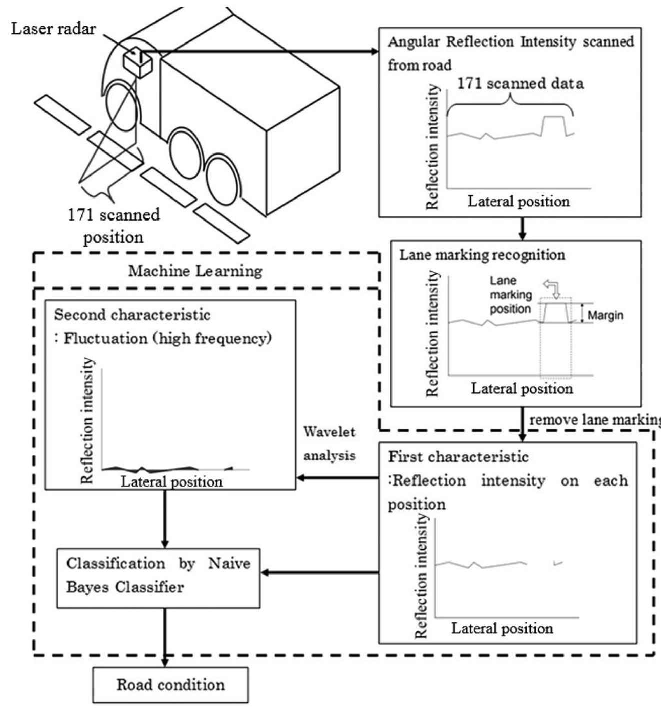


Fig. 14. Signal flow in road surface recognition.

Moreover, to improve the estimation rate, the index of the road surface roughness is used, in addition to the multiple reflection intensities.

When the characteristics of the data have a normal distribution (Gaussian naïve Bayes), the prior distribution $P(x_{f_i}|\mathrm{class})$ can be expressed as follows:

$$P(x_{f_i}|\mathrm{class}_j) = \frac{1}{\sqrt{2\pi\sigma^2_{\mathrm{class}_j,f_i}}} e^{\frac{-\left(x_{f_i} - \mu_{\mathrm{class}_j,f_i}\right)^2}{2\sigma^2_{\mathrm{class}_j,f_i}}}. \quad (2)$$

Here, $\mu_i$ denotes the mean value of feature variable $f_i$ while $\sigma$ denotes the standard deviation of feature variable $f_i$. $n$ denotes the number of feature variables. $x_{f_i}$ denotes a vector of the feature variables. $\mathrm{class}_j$ denotes a class that is classified.

A probability model $P(\mathrm{class}|x_{f_i})$ is calculated using the result of (2)

$$P(\mathrm{class}_j|x_{f_i}) = \frac{P(\mathrm{class}_j)\prod_{i=1}^{n} P(x_{f_i}|\mathrm{class}_j)}{\prod_{i=1}^{n} P(x_i)}. \quad (3)$$

When $C_{NB}$ denotes a discrimination result, the naïve Bayes classifier is shown in (4). This is based on (3), and the maximum probability is classified as the required class

$$C_{NB} = \arg\max_j P(\mathrm{class}_j) \prod_{i=1}^{n} P(x_{f_i}|\mathrm{class}_j). \quad (4)$$

Equation (4), which is the naïve Bayes classifier [35], is calculated online using the training data obtained from the above procedure. Then, the measured road surface is classified according to the six types of road surface.

Fig. 15. Measurement environment.

Fig. 16. Measurement vehicle.

### D. Road Surface Estimation

Road surface estimation is carried out in real time using the scanning data obtained with the laser radar. (In this study, the possibility of road surface estimation in real time was investigated using offline data) The data processing flow is shown in Fig. 14.

(1) The position of a road marking is recognized based on the reflection intensity of the laser radar [30], [31].
(2) The lane marking area is excluded from the road surface estimation area of the scanning area of the laser radar. When the scanning range ($n$ data number) contains lane mark data ($l$ data number) in the scanning range, the reflection intensity data used for estimation is taken away from the number of whole reflection intensities.
(3) The reflection intensities ($n$-$l$ data, here $l$ denotes the number of reflection intensities on the lane mark) and the index of the road surface roughness ($m$ data) is calculated.
(4) The road surface is classified into one of the six road surfaces by using the naïve Bayes classifier Eqs. (2) and (3).

## III. Road Surface Recognition Field Test on Private Road

### A. Construction of Measurement System

In the energy-saving ITS project, the application of sensors to an automatic platoon system was is investigated on a private road provided by Ube Industries, Ltd. (Fig. 15). Tests were run for six months from August 2012 to January 2013 [40]. During this time, a measurement system was installed on the heavy-duty truck (a double-trailer) shown in Figs. 16 and 17. The equipment used in the project is illustrated in Fig. 17. The

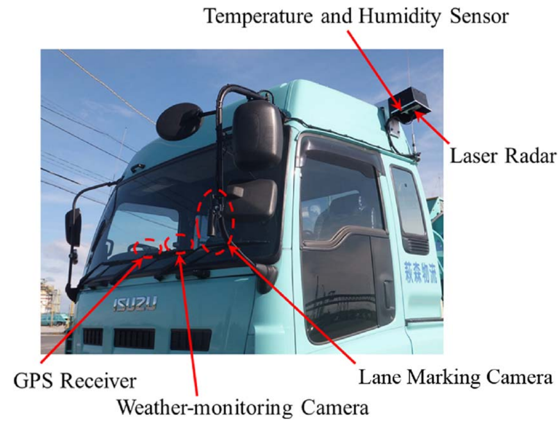


Fig. 17. Sensor system.


Fig. 18. Recognized road surface.

lase r radar used for road surface recognition and lane marking recognition was installed on the left side of the truck's cab. GPS, temperature and humidity sensors, as well as cameras were also installed for collecting weather information and the vehicle's position. In this test, lane marking recognition with laser radar and a camera, as well as road surface recognition, was carried out. For the road surface recognition, only the laser radar was used. If environmental data were to be used for road surface recognition, the recognition rate might improve. However, the purpose of this study was to construct a high-reliability road surface recognition system using only the laser radar. Therefore, only the data from the laser radar was used for road surface recognition in this study.

### B. Laser Radar Measurement of Road Surface

Fig. 18 shows photographs of the six road surface conditions. These are "aged asphalt and dry road surface," "aged asphalt and moist road surface," "aged asphalt and flooded road surface," "new asphalt and dry road surface," "new asphalt and moist road surface," and "new asphalt and flooded road surface."

The measurement vehicle was run at 50 to 60 km/h on the private road (Fig. 15). The sampling frequency of the laser radar was 10 Hz.

An example of the measured data obtained with the laser radar is as shown in Fig. 19. As the vehicle moves forward, the laser scans from the left side of the vehicle. The bright red

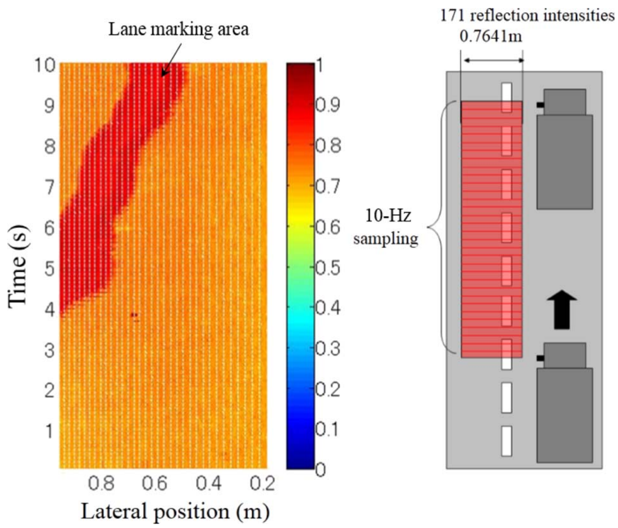


Fig. 19. Measured reflection intensity data.

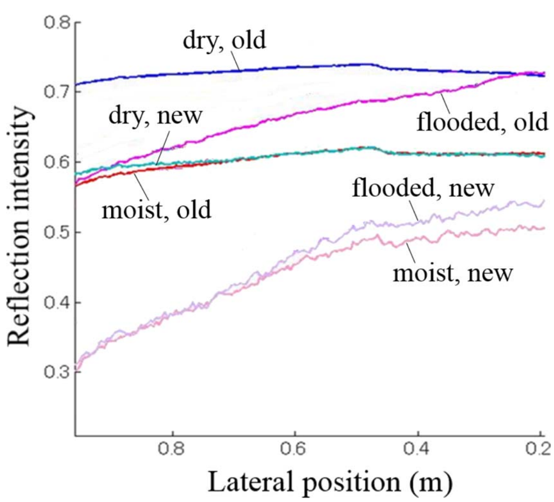


Fig. 20. Measured reflection intensities used as a training data.

area represents highly reflective objects on the road, which are lane markings.

*1) Reflection Intensity:* The reflection intensity (as is shown in Fig. 19) is assembled with a scanning position on the abscissa axis and the reflection intensities on the ordinate axis, as shown in Fig. 20. The means and STDs of the reflection intensity from the six road conditions are shown in Fig. 20. The solid lines represent the mean value. The reflection intensities of the "new asphalt and dry road surface" and "aged asphalt and moist road surface" are very similar. Similarly, the reflection intensity of the "new asphalt and moist road surface" and "new asphalt and flooded road surface" are also very similar. On the other hand, the reflection intensities for the other conditions are quite different. As training data for the machine learning algorithm, the reflection intensities shown in Fig. 20, consisting of 171 reflection intensity points and six road surface conditions, were used.

*2) Index of Road Surface Roughness:* Fig. 20 shows that it is difficult to completely differentiate between the six road surfaces. Therefore, it is necessary to also use the index of the road surface roughness to reliably differentiate between the six road surface conditions. There is one index for the road surface roughness, this being the 172nd feature variable in addition to the 171 reflection intensities. The index of the road surface roughness is calculated in real time from the scanned data.

TABLE I
SPATIAL FREQUENCY RANGE AND WAVELENGTH IN HIGH FREQUENCY SIGNAL OBTAINED BY LEVEL-5 DECOMPOSITION

| Signal | Level of decomposition | Spatial frequency range | Wavelength |
|---|---|---|---|
| D1 | 1 | 74.07 m$^{-1}$ - 148.15 m$^{-1}$ | 6.75 mm – 13.5 mm |
| D2 | 2 | 37.04 m$^{-1}$ - 74.07 m$^{-1}$ | 13.5 mm – 27.0 mm |
| D3 | 3 | 18.52 m$^{-1}$ - 37.04 m$^{-1}$ | 27.0 mm – 54.0 mm |
| D4 | 4 | 9.26 m$^{-1}$ - 18.52 m$^{-1}$ | 54.0 mm – 108.0 mm |
| D5 | 5 | 4.63 m$^{-1}$ - 9.26 m$^{-1}$ | 108.0 mm – 216.0 mm |

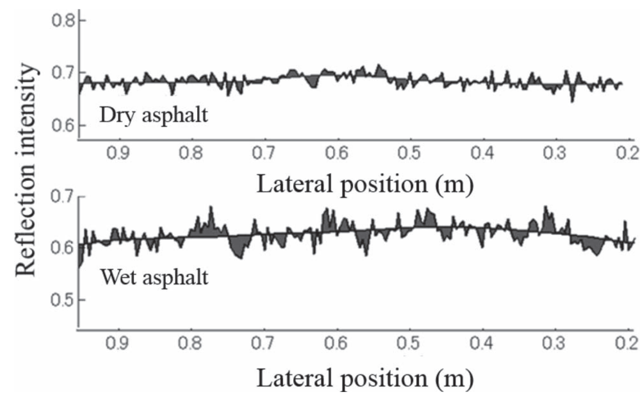


Fig. 21. Fluctuation in dry and moist conditions.

The asperity is extracted from the reflection intensity for each scan using the discrete wavelet transform, and the index of the road surface roughness is calculated. Here, the wavelength of the road asperity is classified from the shortest wavelength D1 to the long wavelength D5. The classified asperity is shown in Table I. Considering the measurement environment, D1, D2, D3, and D4, in which effective information is included, were adopted as a wavelength. The index of the road roughness is defined to summarize the 171 points of the scanning area of D1, D2, D3, and D4. The calculated index for the road roughness is shown in Fig. 21.

The index of the road roughness corresponds to the area of dispersion of the reflection intensity. Training data of the index of road surface roughness is shown in Fig. 22. The training data Figs 20 and 22 are used for the classification of road surface state in the long-term measurement test.

## IV. ROAD SURFACE RECOGNITION RESULTS

To recognize the road surface conditions for the six kinds of road surface states, reflection intensity data for about 1000 s of operation of the vehicle were examined. The vehicle speed was 50 to 60 km/h. The breakdown of the data proved to be "dry and old asphalt: 200 s, 3.3 km," "moist and old asphalt: 200 s, 3.3 km," "flooded and old asphalt: 200 s, 3.3 km," "dry

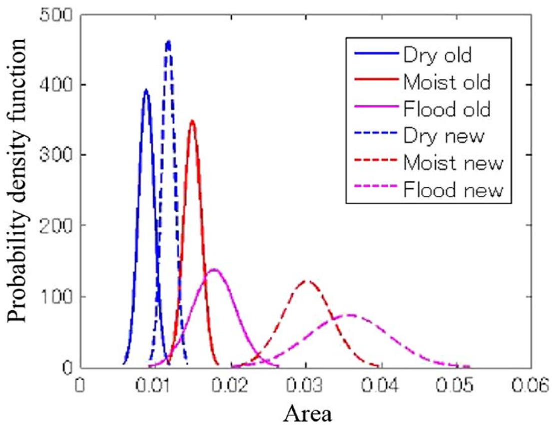


Fig. 22. Index of road surface roughness used as a training data.

TABLE II
PERCENTAGE OF DATA BREAKDOWN

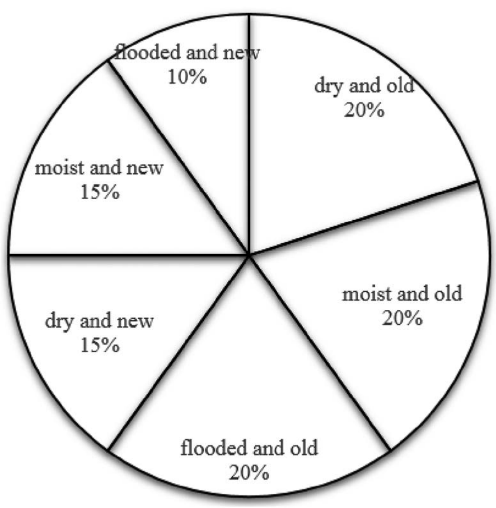


and new asphalt: 150 s, 2.4 km," "moist and new asphalt: 150 s and 2.4 km," and "flooded and new asphalt: 100 s, 1.6 km." The percentage of data breakdown is shown in Table II. Ground truth in each road surface was discriminated based on road colors and weathers by photos of the weather-monitoring camera. It was unable to measure road surface states by using sensing devices because this long-term sensing test was carried out during the operating hours of the private road.

The results of road surface recognition using only multiple reflection intensities determined by the naïve Bayes classifier are shown in Table III. The results of road surface recognition using multiple reflection intensities and the index of the road roughness by the naïve Bayes classifier are shown in Table IV.

When using only multiple reflection intensities, the recognition rate for "moist and aged asphalt" was 27.26% while that for "flooded and new asphalt" was 21.86%. On the other hand, when using multiple reflection intensities and the index of road roughness, the recognition rate for "moist and aged asphalt" was 93.21% while that for "flooded and new asphalt" was 56.43%. When both the multiple reflection intensities and the index of the road roughness were used for road surface recognition, the recognition rate increased substantially. Therefore, we could confirm the efficacy of adding the index of road

TABLE III
RECOGNIZED RESULTS (USING ONLY REFLECTION INTENSITIES)

| Real Condition | Estimated Condition | | | | | |
|---|---|---|---|---|---|---|
| | Dry Old | Moist Old | Flooded Old | Dry New | Moist New | Flooded New |
| Dry old asphalt | **99.35%** | 1% | 0% | 0% | 0% | 0% |
| Moist old asphalt | 0% | **27.26%** | 0.09% | 72.55% | 0.09% | 0% |
| Flooded old asphalt | 0% | 8.91% | **86.20%** | 4.50% | 0% | 0.39% |
| Dry new asphalt | 0.30% | 0. 44% | 0.15% | **99.11%** | 0% | 0% |
| Moist new asphalt | 0.00% | 1.60% | 0.80% | 0% | **93.86%** | 3.74% |
| Flooded new asphalt | 0% | 1% | 0% | 0% | 77.05% | **21.86%** |

TABLE IV
RECOGNIZED RESULTS (PROPOSED METHOD)

| Real Condition | Estimated Condition | | | | | |
|---|---|---|---|---|---|---|
| | Dry Old | Moist Old | Flooded Old | Dry New | Moist New | Flooded New |
| Dry old asphalt | **98.71%** | 0% | 0.46% | 0.83% | 0% | 0% |
| Moist old asphalt | 0% | **93.21%** | 0.57% | 6.04% | 0.19% | 0% |
| Flooded old asphalt | 0% | 15.22% | **82.26%** | 1.50% | 0.47% | 0.55% |
| Dry new asphalt | 4.87% | 0. 86% | 1.18% | **93.06%** | 0% | 0% |
| Moist new asphalt | 0.13% | 1.07% | 1.20% | 0% | **92.92%** | 4.67% |
| Flooded new asphalt | 0% | 0% | 0% | 0% | 43.57% | **56.43%** |

roughness to the feature variable of the naïve Bayes classifier. The recognition rate for new flooded asphalt is still low, however. This may be caused by human error in determining the actual conditions from a picture taken by a camera since it is difficult to distinguish between moist and flooded conditions when using only a camera.

It was possible to attain a 92% recognition rate when attempting to differentiate between dry and moist road surfaces. Moreover, when considering the quality of the road surface, a recognition rate of 92% was achieved when attempting to differentiate between dry and moist road surfaces on new asphalt, while a recognition rate in excess of 93% was attained when attempting to differentiate between a dry and moist road surface on aged asphalt.

In addition, the processing time for the proposed methods was 0.06 s/scanned data. Thus, real-time application is possible.

## V. CONCLUSION

In this study, road surface recognition technology based on laser radar was developed for application to an automatic platooning system. A method of utilizing the laser radar used for lane marking recognition to also recognize the road conditions is proposed. The method uses a machine learning algorithm that is a naïve Bayes classifier. The reflection intensities and fluctuations are used as feature variables. The method also overcomes the problem of the presence/absence of lane markings by utilizing the independent assumption of the naïve Bayes classifier. By using this method, the road surface condition, which is essential to the realization of automatic platooning, can be estimated. For further improvement of a detection rate, it is able to be considered to use a sensor fusion technology obtained from multiple reflection intensities, index of road surface roughness, information from temperature sensor and information from humidity sensor. This is our next step of development of a road surface recognition system.

## ACKNOWLEDGMENT

The measurement test was supported by Ube Industries, Ltd. and Hagimori Logistics, Ltd.

## REFERENCES

[1] S. E. Shladover, "Review of the state of development of Advanced Vehicle Control Systems (AVCS)," *Veh. Syst. Dyn.*, vol. 24, no. 6/7, pp. 551–595, Jul. 1995.
[2] S. Tsugawa, "Survey on automated driving systems," (in Japanese), *IATSS Rev.*, vol. 37, no. 3, pp. 39–47, Jan. 2013.
[3] S. E. Shladover, "PATH at 20—History and major milestones," *IEEE Trans. Intell. Transp. Syst.*, vol. 8, no. 4, pp. 584–592, Dec. 2007.
[4] H. Fritz, "Longitudinal and lateral control of heavy duty trucks for automated vehicle following in mixed traffic: Experimental results from the CHAUFFEUR project," in *Proc. IEEE Int. Conf. Control Appl.*, 1999, pp. 1348–1352.
[5] C. Bergenhem, Q. Huang, A. Benmimoun, and T. Robinson, "Challenges of platooning on public motorways," in *Proc. 17th ITS World Congr.*, 2010, pp. 1–12.
[6] R. Kunze, R. Ramakers, K. Henning, and S. Jeschke, "Organization and operation of electronically coupled truck platoons on German motorways," in *Intelligent Robotics and Applications*, vol. 5928. Berlin, Germany: Springer-Verlag, 1999, pp. 135–146.
[7] T. Mizuma and H. Nakamura "Safety evaluation on automatically operation bus system by its technologies," in *Proc. IEEE Int. Symp. Ind. Electron.*, 2001, pp. 1278–1282.
[8] T. Luettel, M. Himmelsbach, and H. J. Wuensche, "Autonomous ground vehicles—Concepts and a path to the future," *Proc. IEEE*, vol. 100, pp. 1831–1839, May 2012.
[9] M. Campbell, M. Egerstedt, J. P. How, and R. M. Murray,, "Autonomous driving in urban environments: Approaches, lessons and challenges," *Philos. Trans. Roy. Soc. London A, Math. Phys. Sci.*, vol. 368, no. 1928, pp. 4649–4672, Sep. 2010.
[10] K. Aoki and Y. Morita, "Development of automated platooning system based on heavy-duty trucks (first report)," (in Japanese), in *Proc. JSAE Annu. Congr. (Autumn)*, 2009, pp. 1–4.
[11] H. Kawashima, Y. Suzuki, K. Aoki, and Y. Morita, "Development of automated platooning system based on heavy-duty trucks (second report)," (in Japanese), in *Proc. JSAE Annu. Congr. (Spring)*, 2013, pp. 11–14.
[12] M. Aki *et al.*, "Safety testing of an improved brake system for automatic platooning of trucks," *Int. J. Intell. Transp. Syst. Res.*, vol. 12, no. 3, pp. 98–109, Sep. 2014.
[13] F. Gustafsson, "Slip-based tire–road friction estimation," *Automatica*, vol. 33, no. 6, pp. 1087–1099, Jun. 1997.
[14] F. Gustafsson, "Monitoring tire–road friction using the wheel slip," *IEEE Control Syst.*, vol. 18, no. 4, pp. 42–49, Aug. 1998.
[15] J. O. Hahn, R. Rajamani, and L. Alexander, "GPS-based real-time identification of tire-road friction coefficient," *IEEE Control Syst. Technol.*, vol. 10, no. 3, pp. 331–343, May 2002.
[16] S. Muller, M. Uchanski, and K. Hedrick, "Estimation of the maximum tire–road friction coefficient," *Trans. ASME, J. Dyn. Syst. Meas. Control*, vol. 125, no. 4, pp. 607–617, Jan. 2003.
[17] L. Alvarez, J. Yi, R. Horowitz, and L. Olmos, "Dynamic friction model-based tire–road friction estimation and emergency braking control," *Trans. ASME, J. Dyn. Syst. Meas. Control*, vol. 127, no. 1, pp. 22–32, Mar. 2005.
[18] G. Baffet, A. Charara, and G. Dherbomez, "An observer of tire–road forces and friction for active security vehicle systems," *IEEE/ASME Trans. Mechatronics*, vol. 12, no. 6, pp. 651–661, Dec. 2007.
[19] Friction Project. [Online]. Available: http://friction.vtt.fi/.
[20] T. Haas *et al.*, "Fusion of vehicle and environment sensing in friction project," *Proc. 17th Aachen Colloq. Autom. Engine Technol. Congr.*, Aachen, Germany, Oct. 2008.
[21] R. Rajamani, D. Piyabongkarn, J. Y. Lew, K. Yi, and G. Phanomchoeng, "Tire–road friction-coefficient estimation," *IEEE Control Syst. Mag.*, vol. 30, no. 4, pp. 54–69, Aug. 2010.
[22] G. Erdogan, L. Alexander, and R. Rajamani, "Estimation of tire–road friction coefficient using a novel wireless piezoelectric tire sensor," *IEEE Sensors J.*, vol. 11, no. 2, pp. 267–269, Feb. 2011.
[23] R. Rajamani, G. Phanomchoeng, D. Piyabongkarn, and J. Y. Lew, "Algorithms for real-time estimation of individual wheel tire–road friction coefficients," *IEEE/ASME Trans. Mechatronics*, vol. 17, no. 6, pp. 1183–1195, Dec. 2012.
[24] F. Holzwarth and U. Eichhorn, "Non-contact sensors for road conditions," *Sens. Actuators A, Phys.*, vol. 37/38, pp. 121–127, Jun. 1993.
[25] T. Ogura *et al.*, "Study on a road surface sensing system for snow and ice road," *JSAE Rev.*, vol. 23, no. 3, pp. 333–339, Jul. 2002.
[26] M. Yamada, T. Oshima, K. Ueda, I. Horiba, and S. Yamamoto, "A study of the road surface condition detection technique for deployment on a vehicle," *JSAE Rev.*, vol. 24, no. 2, pp. 183–188, Apr. 2003.
[27] J. Casselgren, M. Sjödahl, and J. Leblanc, "Angular spectral response from covered asphalt," *Appl. Opt.*, vol. 46, no. 2, pp. 4277–4288, Jul. 2007.
[28] J. Casselgren, M. Sjödahl, M. Sanfridsson, and S. Woxneryd, "Classification of road conditions—To improve safety," in *Advanced Microsystems for Automotive Applications*, J. Valldorf and W. Gessner, Eds. Berlin, Germany: Springer-Verlag, 2007, pp. 47–59.
[29] M. Jokela, M. Kutila, and L. Le, "Road condition monitoring system based on a stereo camera," in *Proc. IEEE 5th Int. Conf. ICCP*, Aug. 2009, pp. 423–428.
[30] M. Matsuura, T. Isogai, and H. Akatsuka, "Lane recognition system using laser radar for platooning—Development of energy-saving ITS technologies," in (in Japanese) *Proc. JSAE Annu. Congr. (Spring)*, 2010, pp. 5–8.
[31] M. Matsuura, T. Isogai, and T. Kawai, "Lane recognition system using laser radar for platooning (Report No. 2)—Development of energy-saving ITS technologies," (in Japanese) in *Proc. JSAE Annu. Congr. (Autumn)*, 2010, pp. 1–3.
[32] T. Ogawa and K. Takagi, "Lane recognition using on-vehicle LIDER," in *Proc. IEEE Intell. Veh. Symp.*, 2006, pp. 540–545.
[33] K. Takagi, K. Morikawa, T. Ogawa, and M. Saburi, "Road environment recognition using on-vehicle LIDER," in *Proc. IEEE Intell. Veh. Symp.*, 2006, pp. 120–125.
[34] V. P. Tolstoy, I. Chernyshova, and V. A. Skryshevsky, *Handbook of Infrared Spectroscopy of Ultrathin Films*. Weinheim, Germany: Wiley-VCH, 2003.
[35] T. Hastie, R. Tibshirani, and J. Friedman, *The Elements of Statistical Learning: Data Mining, Inference, and Prediction, Second Edition*. New York, NY, USA: Springer-Verlag, 2009.
[36] Y. Liu and H. Shi, "Naïve Bayes vs. support vector machine: Resilience to missing data," in *Proc. 3rd Int. Conf. Artif. Intell. Comput. Intell.*, 2011, vol. 2, pp. 680–687.
[37] M. Martinez-Arroyo and L. E. Sucar, "Learning an optimal naive Bayes classifier," in *Proc. 18th Int. Conf. Pattern Recognit.*, 2006, pp. 1236–1239.
[38] S. Mallat, "A theory for multi-resolution signal decomposition: The wavelet representation," *IEEE Trans. Pattern Anal. Mach. Intell.*, vol. 11, no. 7, pp. 674–693, Jul. 1989.
[39] G. Strang and T. Nguyen, *Wavelets and Filter Banks*. Cambridge, MA, USA: Wellesley-Cambridge, 1997.
[40] M. Aki *et al.*, "Field operation test of sensing system and ECU function for automatic driving of trailer-type truck," in *Proc. ITS World Congr. Tokyo*, 2013, pp. 1–12.

**Masahiko Aki** received the Bachelor's, Master's, and Doctorate degrees from Nihon University, Tokyo, Japan, in 2004, 2006, and 2009, respectively, all in mechanical engineering. From 2009 to 2012 and from 2012 to 2013, he was a Project Researcher and a Project Research Associate, respectively, with the Institute of Industrial Science, The University of Tokyo. Since 2013, he has been an Assistant Professor with Nagoya University, Nagoya, Japan. His major research interests are the dynamics and control of vehicle systems.

**Teerapat Rojanaarpa** received the M.E. degree in mechanical engineering from The University of Tokyo, Tokyo, Japan, in 2012. His major fields are machine learning and pattern recognition. Since 2013, he has been with DENSO Corporation, Aichi, Japan, where he is currently a Researcher at the Advance R&D Center.

**Kimihiko Nakano** received the Bachelor's, Master's, and Doctorate degrees from The University of Tokyo, Tokyo, Japan, in 1995, 1997, and 2000, respectively, all in mechanical engineering. He is currently an Associate Professor at The University of Tokyo. His major research interests are the dynamics and control of vehicles and human factors in driving.

**Yoshihiro Suda** received the D.Eng. degree from The University of Tokyo, Tokyo, Japan, in 1987. He is currently a Professor in the Institute of Industrial Science and the Director of the Advanced Mobility Research Center at The University of Tokyo. His major fields are vehicle dynamics and control. He is a Board Member of ITS Japan, a Member of ASME and SICE, and a Fellow of JSME and JSAE.

**Naohito Takasuka** received the Master's degree in information science and technology from Hokkaido University, Sapporo, Japan, in 2011. His major fields are computer vision and pattern recognition. Since 2011, he has been with DENSO Corporation, Aichi, Japan, where he is currently a Researcher at Nippon Soken Inc.

**Toshiki Isogai** received the Bachelor's degree in materials science and engineering from Nagoya University, Nagoya, Japan, in 1991. His major fields are computer vision and pattern recognition. He is currently a Project Manager with the Technology Planning Department, DENSO Corporation, Aichi, Japan.

**Takeo Kawai** received the Bachelor's degree in electronics engineering from Waseda University, Tokyo, Japan, in 1980. He is currently a Project Director with the Technology Planning Department, DENSO Corporation, Aichi, Japan.